



Delhi Technological University

(Formerly Delhi College of Engineering)

Bawana Road, Delhi-110042

Department of Applied Physics

**GREEN SYNTHESIZED
SILVER NANOPARTICLES: SURFACE
PLASMON RESONANCE ALLIED
APPLICATIONS**

A DISSERTATION THESIS SUBMITTED FOR PARTIAL FULFILLMENT OF THE
REQUIREMENTS FOR RECEIVING DEGREE OF MASTER'S IN PHYSICS

Submitted by:

Samiksha Shukla (2K20/MSCPHY/28)

Under the supervision of:

Dr. Mohan Singh Mehata

CANDIDATE'S DECLARATION

I, Samiksha Shukla (Roll Number: 2K20/MSCPHY/28), student of M.Sc. (Applied Physics), hereby declare that dissertation project titled “Green synthesized silver nanoparticles: surface plasmon resonance allied applications”, submitted to the Department of Applied Physics, Delhi Technological University in partial fulfilment of the requirement for the award of the degree of Masters in Applied Physics is an authentic work where all sources used have been rightfully cited. This work has not been used previously during any degree, diploma, or fellowship.

1. Paper published in Scopus indexed journal with following details:

Title of Paper: “Catalytic activity of Green synthesized Silver Nanoparticles using Crinum asiaticum (Sudarshan) leaf extract”

Authors names (in sequence as per research paper): Samiksha Shukla, Anne Masih, Aryan, Mohan Singh Mehata

Name of the conference: Materials Today: Proceedings

Status of paper: Published

Date of communication: 15th November 2021

Date of acceptance: 26th December 2021

Available online: 11th January 2022

Published on: 18th April 2022

2. Work under review in Science citation index expanded journal with following details:

Title of Paper: “Selective picomolar detection of carcinogenic chromium ions using biosynthesized silver nanoparticles and their enhanced antibacterial activity”

Authors names (in sequence as per research paper): Samiksha Shukla, Mohan Singh Mehata

Name of the journal: Materials Today: Sustainability

Status of paper (Accepted/published/communicated): Communicated - Under review

Review(s) completed: 1

Review(s) awaited: 1

Date of communication: 24th April 2022

Place: New Delhi

Date: 10 May 2022



Samiksha Shukla

Dr. Mohan Singh Mehata
Former JSPS (Japan) and CAS (China) Fellow

Assistant Professor



Department of Applied Physics
Delhi Technological University

Bawana Road, Delhi 110042
INDIA

Mob: +91-9953142553

Email: msmehata@dtu.ac.in
msmehata@gmail.com

SUPERVISOR CERTIFICATE

I, hereby certify that the project dissertation titled “Green synthesized silver nanoparticles: surface plasmon resonance allied applications”, by Samiksha Shukla (Roll No. 2K20/MSCPHY/28) submitted to the Department of Applied Physics, Delhi Technological University in partial fulfilment of the requirement for the award of the degree of Masters in Applied Physics, is a record of the project work carried out by the student under my supervision. This work has not been submitted partially or completely during any degree or diploma to this university or anywhere else, to the best of my knowledge.

Place: New Delhi

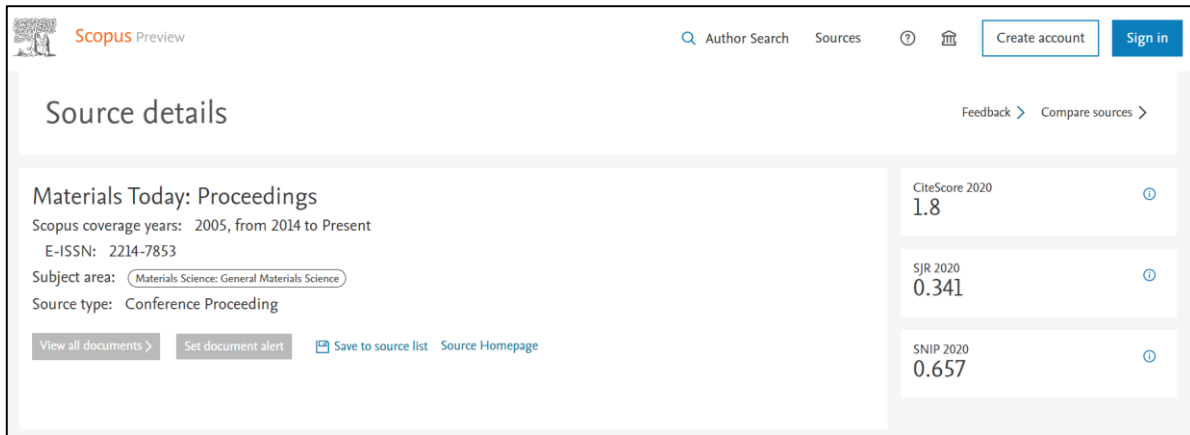
Date: 10 May 2022

Dr. Mohan Singh Mehata

Supervisor

PROOF OF INDEXING

1. Materials Today: Proceedings



Scopus Preview

Author Search Sources ⓘ ⓘ Create account Sign in

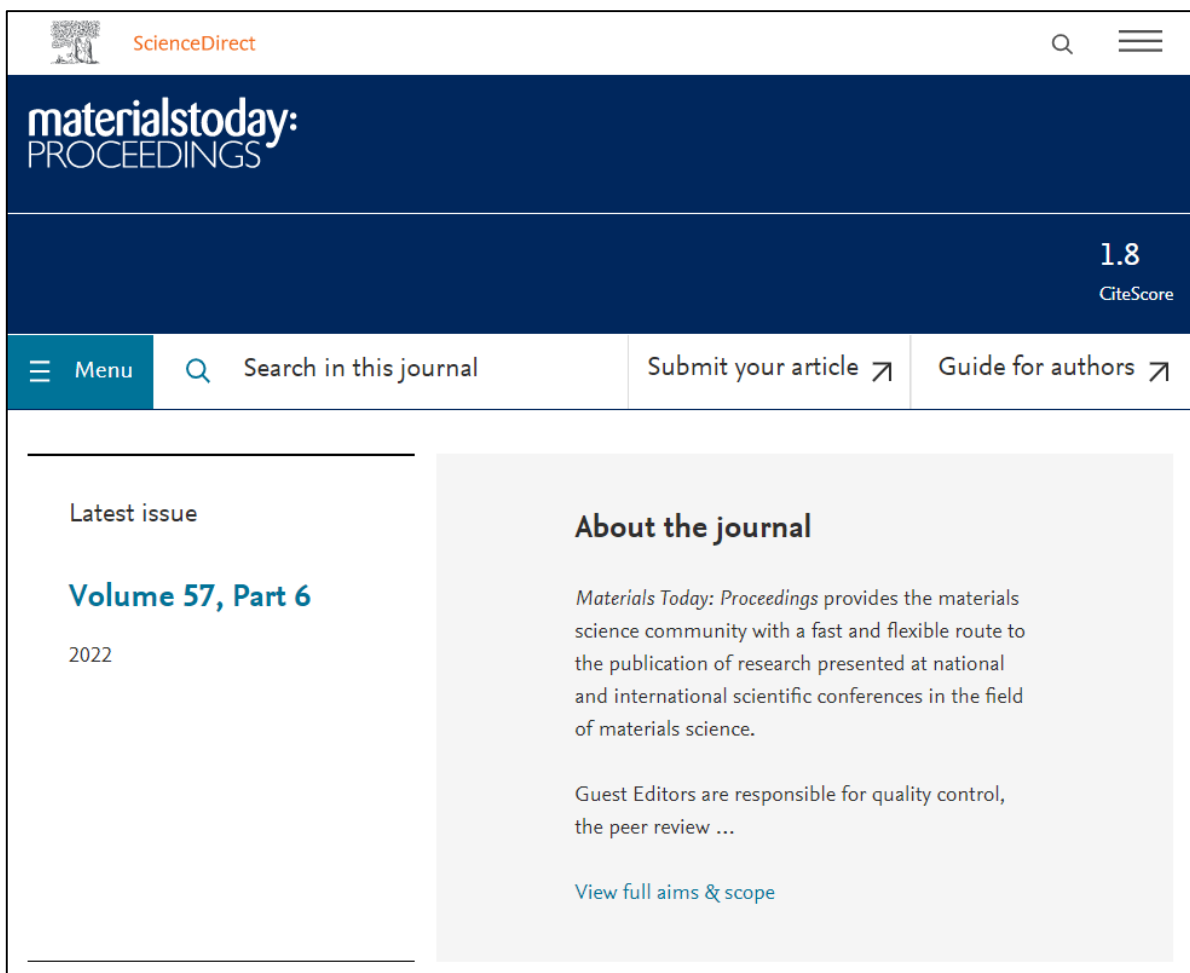
Source details

Feedback > Compare sources >

Materials Today: Proceedings
Scopus coverage years: 2005, from 2014 to Present
E-ISSN: 2214-7853
Subject area: [Materials Science: General Materials Science](#)
Source type: Conference Proceeding

[View all documents >](#) [Set document alert](#) [Save to source list](#) [Source Homepage](#)

CiteScore 2020	1.8	ⓘ
SJR 2020	0.341	ⓘ
SNIP 2020	0.657	ⓘ



ScienceDirect

materialstoday: PROCEEDINGS

1.8 CiteScore

Menu Search in this journal Submit your article ↗ Guide for authors ↗

Latest issue

Volume 57, Part 6

2022

About the journal

Materials Today: Proceedings provides the materials science community with a fast and flexible route to the publication of research presented at national and international scientific conferences in the field of materials science.

Guest Editors are responsible for quality control, the peer review ...

[View full aims & scope](#)

2. Materials Today: Sustainability

The screenshot shows the journal's homepage on ScienceDirect. At the top left is the ScienceDirect logo. To its right are the links 'Journals & Books', a search icon, and buttons for 'Register' and 'Sign in'. Below this is a dark blue header banner. On the left of the banner is the journal's cover image with the text 'materialstoday SUSTAINABILITY'. To the right of the cover, the journal title 'Materials Today Sustainability' is displayed, along with the text 'Supports open access'. Further right, the journal's metrics are shown: '2.9 CiteScore' and '4.524 Impact Factor'. Below the banner is a navigation bar with dropdown menus for 'Articles & Issues', 'About', and 'Publish', a search box labeled 'Search in this journal', and links for 'Submit your article' and 'Guide for authors'. The main content area is split into two columns. The left column contains a sidebar with links for 'Aims and scope', 'Editorial board', 'Abstrating & indexing' (which is underlined), and 'News'. The right column is titled 'Abstrating & indexing' and contains a bulleted list of indexing services: 'Current Contents - Agriculture, Biology & Environmental Sciences', 'Current Contents - Engineering, Computing & Technology', 'Current Contents - Physical, Chemical & Earth Sciences', 'Essential Science Indicators', 'INSPEC', 'Journal Citation Reports - Science Edition', and 'Science Citation Index Expanded'.

ScienceDirect Journals & Books Register Sign in

materialstoday SUSTAINABILITY

Materials Today Sustainability Supports open access

2.9 CiteScore | 4.524 Impact Factor

Articles & Issues About Publish Search in this journal Submit your article Guide for authors

Aims and scope
Editorial board
Abstrating & indexing
News

Abstrating & indexing

- Current Contents - Agriculture, Biology & Environmental Sciences
- Current Contents - Engineering, Computing & Technology
- Current Contents - Physical, Chemical & Earth Sciences
- Essential Science Indicators
- INSPEC
- Journal Citation Reports - Science Edition
- Science Citation Index Expanded

PLAGIARISM REPORT

WORD COUNT

8195 Words

CHARACTER COUNT

49266 Characters

PAGE COUNT

52 Pages

FILE SIZE

3.7MB

SUBMISSION DATE

May 10, 2022 1:12 AM GMT+5:30

REPORT DATE

May 10, 2022 1:16 AM GMT+5:30

● 9% Overall Similarity

The combined total of all matches, including overlapping sources, for each database.

- 7% Internet database
- 3% Publications database
- Crossref database
- Crossref Posted Content database
- 5% Submitted Works database

● Excluded from Similarity Report

- Bibliographic material
- Cited material
- Small Matches (Less than 10 words)

● 9% Overall Similarity

Top sources found in the following databases:

- 7% Internet database
- 3% Publications database
- Crossref database
- Crossref Posted Content database
- 5% Submitted Works database

TOP SOURCES

The sources with the highest number of matches within the submission. Overlapping sources will not be displayed.

1	dspace.dtu.ac.in:8080 Internet	1%
2	Kookmin University on 2020-06-02 Submitted works	<1%
3	VIT University on 2015-07-22 Submitted works	<1%
4	dspace.dtu.ac.in:8080 Internet	<1%
5	IIT Delhi on 2019-05-28 Submitted works	<1%
6	academic-accelerator.com Internet	<1%
7	Dubai International Academy on 2011-10-18 Submitted works	<1%
8	akademiabaru.com Internet	<1%

9	iaeme.com Internet	<1%
10	Delhi Technological University on 2019-04-02 Submitted works	<1%
11	V.V.S. Sricharan, Srinivasan Chandrasekaran. "Time-domain analysis o... Crossref	<1%
12	Ruby, Aryan, Mohan Singh Mehata. " Surface plasmon resonance allie... Crossref	<1%
13	dokumen.pub Internet	<1%
14	es.scribd.com Internet	<1%
15	journals.plos.org Internet	<1%
16	vignan.ac.in Internet	<1%
17	Aston University on 2020-04-09 Submitted works	<1%
18	Kumar, C. Senthil, M.D. Raja, D. Sathish Sundar, M. Gover Antoniraj, an... Crossref	<1%
19	Pondicherry University on 2012-12-05 Submitted works	<1%
20	University of Strathclyde on 2021-04-12 Submitted works	<1%

21	mafiadoc.com	Internet	<1%
22	ouci.dntb.gov.ua	Internet	<1%
23	mdpi.com	Internet	<1%
24	Muhammad Ismail, M.I. Khan, Kalsoom Akhtar, Murad Ali Khan, Abdull...	Crossref	<1%
25	Naiyf S. Alharbi, Marimuthu Govindarajan, Shine Kadaikunnan, Jamal ...	Crossref	<1%
26	docksci.com	Internet	<1%
27	docplayer.net	Internet	<1%
28	eprints.lums.ac.ir	Internet	<1%
29	hdl.handle.net	Internet	<1%
30	onlinelibrary.wiley.com	Internet	<1%
31	pubs.rsc.org	Internet	<1%
32	web.archive.org	Internet	<1%
33	hindawi.com	Internet	<1%

Place: New Delhi

Date: 10 May 2022



Samiksha Shukla



SUPERVISOR SIGN

ACKNOWLEDGEMENT

Foremost, I would express my indebtedness and deepest sense of regard to my supervisor, Dr. Mohan Singh Mehata, Assistant Professor, Department of Applied Physics, Delhi Technological University for providing his incessant expertise, inspiration, encouragement, suggestions, and this opportunity to work under his guidance. I am grateful for the constant help provided at every step of this project by all the lab members (PhD scholars) of Laser Spectroscopy Laboratory, Department of Applied Physics, Delhi Technological University. I am also thankful to my family, co-authors and colleagues for their invaluable support, care and patience during this project. Lastly, I would thank Delhi Technological University for providing such a wonderful opportunity of working on this project.

ABSTRACT

For this study, biocompatible silver nanoparticles (Ag-NPs) were successfully synthesized via employing an environment friendly green approach by usage of flower extract of *Plumeria obtusa*. For studying the attributes of synthesized Ag-NPs, techniques such as UV-vis spectroscopy, X-Ray diffractometry (XRD), transmission electron microscopy (TEM), zeta potential and dynamic light scattering (DLS) analysis were used. The characteristic surface plasmon resonance (SPR) peak of Ag-NPs was observed around 430 nm. This peak was found to be dependent on different physicochemical parameters like amount of flower extract, reaction time, temperature and pH value. The crystal structure was studied from XRD pattern which confirmed the formation of FCC lattice with a crystallite size of 20 nm and particle size of 14 nm. TEM analysis also showed that spherical Ag-NPs of mean diameter 13 nm were formed. The stability of colloidal Ag-NPs was studied using zeta potential analysis, whose value came out to be 13 nm. The synthesized Ag-NPs were used in developing a sensing mechanism for a very harmful carcinogen, hexavalent chromium (Cr^{6+}) and the same was tested in three different aqueous mediums. The limit of detection (LoD) came out to be 95 ± 2 pM, which is lowest reported value of LoD for a biosynthesized nanomaterials and thus, can be efficiently applied in diagnosing any contamination by cancer-causing Cr^{6+} , in drinking water or food. Further, the enhancement in anti-bacterial action of Ag-NPs over AgNO_3 was also investigated, against a gram-positive bacterium, *S. Aureus*. The inhibition zone came out to be much wider (10.8 mm) than that of AgNO_3 (7.7 mm) or plant extract (6.7 mm). Thus, the Ag-NPs synthesized in this project are non-toxic, cost-efficient and can be utilized in a variety of applications like biosensing and biomedicine.

CONTENTS

Cover page	i	
Candidate's Declaration	ii	
Supervisor Certificate	iv	
Proof of Scopus Indexing	v	
Plagiarism Report	vii	
Acknowledgement	ix	
Abstract	x	
Contents	xi	
List of Figures	xiv	
List of Tables	xv	
List of Symbols and abbreviations	xvi	
CHAPTER 1	INTRODUCTION	1-5
1.1	Nanotechnology	
1.2	Literature review	
1.2.1	Synthesis of nanoparticles	
1.2.1.1	Physical synthesis	
1.2.1.2	Chemical synthesis	
1.2.1.3	Green synthesis	
1.2.2	Silver Nanoparticles	
1.3	Plant Used	
1.4	Enhanced Anti-bacterial action of Ag-NPs	
1.5	Selective sensing property towards carcinogenic Cr ⁶⁺	
1.6	Aim and scope of study	

CHAPTER 2	MATERIALS AND METHODS	6-7
2.1 Materials used		
2.2 Plant used		
2.3 Synthesis of Ag-NPs		
CHAPTER 3	CHARACTERIZATION TECHNIQUES	8-10
3.1 UV/VIS/NIR spectroscopy		
3.2 X-ray diffraction		
3.3 TEM Analysis		
3.4 Zeta potential		
CHAPTER 4	RESULT AND DISCUSSIONS	11- 20
4.1 Absorption Spectra		
4.1.1 Influence of amount of flower extract on synthesis		
4.1.2 Influence of time		
4.1.3 Influence of reaction temperature		
4.1.4 Influence of pH		
4.2 XRD Pattern		
4.3 Morphology		
4.4 Zeta potential analysis		
4.5 Selective sensing towards carcinogenic Cr ⁶⁺		
CHAPTER 5	CONCLUSION	21

APPENDIX	22
RESEARCH PAPERS	23
REFERENCES	24-32

LIST OF FIGURES

Figure 1. Pictorial illustration of mechanism behind biosynthesizing Ag-NPs

Figure 2. Biosynthesis of Ag-NPs from prepared flower essence of *Plumeria obtusa*

Figure 3. Perkin Elmer Lambda™ 750 UV/Vis/NIR spectrophotometer

Figure 4. Bruker's D-8 Advanced X-Ray Diffractometer

Figure 5. Morgagni 268D Transmission Electron Microscope

Figure 6. Zetasizer Nano ZS by Malvern

Figure 7. Absorption spectra for colloidal Ag-NPs along with AgNO₃ and prepared flower extract (a) influence of variation of extract concentration (b), the influence of time (c), the influence of temperature variation (d) and the influence of pH variation (e).

Figure 8. XRD pattern for Ag-NPs thin film.

Figure 9. TEM image observed for Ag-NPs (a) Particle size distribution (b)

Figure 10. Hydrodynamic size distribution by intensity, repeated for 3 records. Inset represents the apparent zeta potential (mV) of colloidal Ag-NPs.

Figure 11. Antibacterial action of Ag-NPs (a), flower extract (b), Ag-NPs (c) and Ag-NO₃ against *S. Aureus* (d).

Figure 12. Colour changes in colloidal Ag-NPs after adding different metal ions (166.6 nM)

Figure 13. Absorption spectra of colloidal Ag-NPs post addition of various metal ions, inset represents a bar diagram for ratio of peak absorbances of different metal ions to pure Ag-NPs (a), successive addition of Cr⁶⁺ ions in aqueous medium of deionized water (b), tap water (c) and Yamuna river water (d). Inset shows linearity of 1/absorbance of Cr⁶⁺ treated Ag-NPs as a function of concentration of Cr⁶⁺.

Figure 14. Graphical Abstract

Figure SD1. EDAX for synthesized Ag-NPs

LIST OF TABLES

Table 1. Physical properties of Silver

Table 2. Bragg's reflection peaks for Ag-NPs

Table 3. Inhibition zone in *S. Aureus* treated with flower extract, Ag-NPs and AgNO₃

Table 4. Correlation factor and LoD for detection of Cr⁶⁺ in different aq. mediums

Table 5. Comparison of previously reported nanosensors for Cr⁶⁺ detection.

Table SD₁. Parameters of Ag-NPs recorded on thin film

LIST OF SYMBOLS AND ABBREVIATIONS

NPs	Nanoparticles
Ag	Silver
Ag-NPs	Silver nanoparticles
XRD	X-Ray Diffraction
TEM	Transmission electron microscopy
DLS	Dynamic light scattering
SPR	Surface Plasmon Resonance
FCC	Face centered cubic
LoD	Limit of detection
AgNO ₃	Silver Nitrate
Chromium	Cr
DNA	Deoxyribonucleic acid
UV-Vis	Ultraviolet-Visible
NIR	Near Infrared Spectroscopy
FWHM	Full Width Half Maxima
UP	Ultrapure
SPR	Surface Plasma Resonance
v/v	Volume by volume
JCPDS	Joint Committee on Powder Diffraction Standards
Ag ₂ Cr ₂ O ₇	Silver dichromate

CHAPTER 1

INTRODUCTION

1.1 NANOTECHNOLOGY

Nanotechnology or nanotech is the science and engineering of understanding and controlling matter at the nanoscale (approximately between 1 nm and 100 nm), where their exceptionally small size enables multitudinal novel applications. ‘Nano’ in nanotech comes from the Greek word ‘nanos’ meaning small. A nanometer is about a billionth of a meter. Particles or materials of sizes 1-100 nm are typically called nanoparticles or nanomaterials. Most applications involving nanotechnology are based on the unique set of properties exhibited by nanosized materials, including high surface to volume ratio and nano-size effects. However, the conventional synthesis methods of nanomaterials pose new health and environmental hazards.

1.2 LITERATURE REVIEW

1.2.1 Synthesis of nanoparticles

The interest in the methods of synthesizing metallic nanoparticles is increasing successively these days, owing to their antimicrobial, cytotoxic, optical and various other properties [1–8]. This is mostly because of the variety of disciplines where metal nanoparticles can be effectively used. The most common methods of synthesis of metal nanoparticles can be broadly classified into three main categories.

1.2.1.1 Physical Synthesis

The two key physical approaches of synthesis are Evaporation Condensation and Laser Ablation. However, the physical synthesis methods often occupy large spaces, exhaust huge amounts of energy, involve raising the temperature around the source material to very high values, and require a lot of time to achieve thermal stability [9].

1.2.1.2 Chemical Synthesis

The basic mechanism of chemical synthesis is reduction of Ag^+ ions to Ag^0 and then prevention of any deposition or aggregation using suitable stabilizers, capping agents and surfactants, often polymeric compounds [10]. However, such typical synthetic precursors lead to toxicity in the samples, high production costs and unfortunate effects on environment.

1.2.1.3 Green Synthesis

In green synthesis, green agents (plants or microorganisms) are used for capping and reducing of Ag^+ ions [11,12]. Despite the fact that the exact synthesis mechanism behind green route hasn't been completely acknowledged, but certain compounds present in plants, like alkaloids, phenols, terpenoids, flavonoids and proteins [13] are considered the basis of reduction and capping of Ag-NPs. In case of microorganism mediated green synthesis [14], the antioxidant and reducing properties of microbes govern the reduction process but it requires the need of maintaining elaborate microbe cell cultures and aseptic environments. Hence, green synthesis of Ag-NPs using plant extracts is an efficient eco-friendly one-step alternative to complex physical and chemical routes that doesn't require any challenging high pressurized or high temperature conditions. The samples generated from green methods are non-toxic and economical and hence, can be used in the field of biology.

1.2.2 Silver Nanoparticles

Silver (Ag) is a soft, white, reflective, ductile, malleable, lustrous transition metal with great conductivities, electrical as well as thermal. has been recognized as a precious noble metal since ancient times, on grounds of its anti-corrosive and medicinal behaviour [15]. Ag is being used in medical sciences since the classical age [16]. However, the future scope of Ag for diagnostic, medicinal and therapeutic practices lies strictly in nanoscales as the nanoparticles of Ag act as photocatalysts [17,18], antibacterial, antimicrobial, antioxidant, antiplatelet, antidiabetic, antithrombotic agents [19–24] and in targeted drug delivery systems [25,26]. When the

interaction of free electrons present at the Ag-NPs surface is effectuated at certain wavelengths, the electrons oscillate collectively, giving rise to SPR. Because of this property, Ag-NPs show exceptional absorption and scattering efficiency of light. Thus, the synthesis process of Ag-NPs involves a visual indicator, that is, the colourless precursor solution of silver nitrate (AgNO_3) becoming completely brown owing to SPR, as Ag-NPs are formed [27].

Table 1. Physical properties of Silver

Atomic Mass:	107.87 amu
Atomic Number:	47
Electronic Configuration:	$[\text{Kr}]4d^{10}5s^1$
Melting Point:	961.8 °C
Density:	10.49 g/cm ³

1.3 PLANT USED

For this study, the flowers of *Plumeria obtusa* plant were used. It is popularly known as *Champa* and is of great importance in terms of religion, pharmacology and medicine in India [28]. Other than being used as an ornamental plant for its pleasant fragrance and visual appeal, the flowers of this plant are also actively used in treatment of diseases like diabetes mellitus and in aromatherapy [29]. This particular plant was selected for this study since, it is available in abundance and contains various phytochemicals like terpenoids, flavonoids and phenolic acids [30,31], necessary for acting as a reducer and stabilizer. The essence procured from the flowers of *Plumeria obtusa* was taken to be used as the reducing and capping agent in the preparation of Ag-NPs. Figure 1 schematically explains the mechanism behind synthesis of Ag-NPs via the phytochemicals present in flower essence of *Plumeria obtusa*.

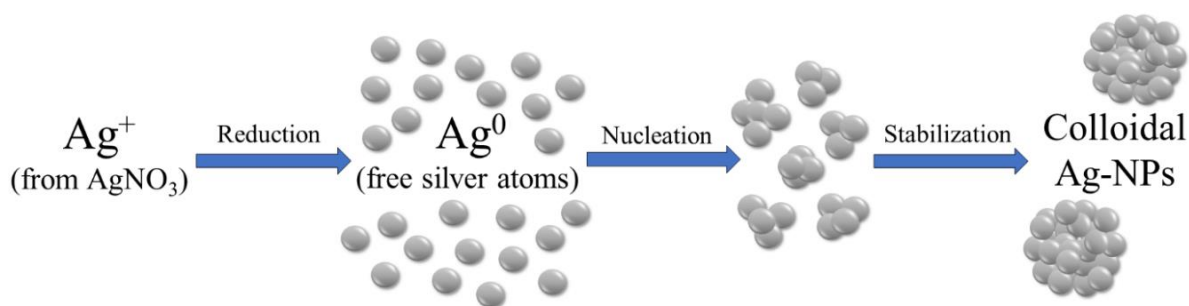


Figure 1. Pictorial illustration of mechanism behind biosynthesizing Ag-NPs

1.4 ENHANCED ANTI-BACTERIAL ACTION OF Ag-NPs

The increasing use of anti-biotics has led to emergence of a new problem, multidrug resistance. For solving the same, new anti-bacterial strategies must be formulated. Silver has been highly regarded anti-microbial agent since classical ages. Ionized Ag in AgNO_3 shows very high binding affinity towards the bacteria's proteins, DNA and RNA which forms the basis for its anti-bacterial action. Since nanoparticles of Ag have much larger surface area per unit volume than ionized Ag in AgNO_3 , they provide better contact with the surface of bacteria and hence, lead to enhancement in the anti-bacterial action. Bacteria are either gram-positive or gram-negative. Gram-positive bacteria have thicker peptidoglycan layer than gram-negative bacteria. For this study, a gram-positive bacteria *Staphylococcus aureus* was taken for investigating the enhanced anti-bacterial action of Ag-NPs. *S. Aureus* is known to be a leading cause of numerous skin and tissue diseases like boils and cellulitis and also, Pneumonia.

1.5 SELECTIVE SENSING PROPERTY TOWARDS CARCINOGENIC Cr^{6+}

The average contemporary living standards of humans often involve exposures to toxic heavy metals and carcinogenic materials like chromium. Their widespread commercial use makes water bodies and food items more prone to contamination, any contact or infestation of them may lead to oxidative stress, cancer related diseases and damage to DNA present in cells [32]. Heavy metal chromium (Cr) exists majorly in 4 oxidation states, elemental, divalent, trivalent

and hexavalent (0, +2, +3 and +6, respectively). Cr in its hexavalent state is a very strong carcinogen. Its toxicity lies behind its reduction mechanism, by release of reactive hydroxyl radicals, that cause permanent cell and DNA damage [33]. Early detection of cancer-causing food or water contaminated by carcinogens like Cr^{6+} is way more ideal than resorting to expensive cancer treatments. Initially for a few years, the only available detection method was through rodents [34,35]. Now, more techniques such as isotope dilution analysis [36], atomic absorption spectrometry [37,38] and ion chromatography [39] have been developed. Although they are reliable, technologically advanced and evolved but they are also complicated and expensive. Therefore, newer and simpler detection strategies involving chemical or optical sensors based on biocompatible nanoparticles of noble metals such as silver and gold, especially for aqueous mediums are being researched [40,41].

1.6 AIM AND SCOPE OF STUDY

- Environment friendly synthesis of biocompatible Ag-NPs via plant extract, controlled by physicochemical parameters.
- Analysing the crystal structure, morphology, stability and polydispersity of the developed Ag-NPs by different characterization techniques.
- Investigating enhanced anti-bacterial action of Ag-NPs against gram-positive bacterial strains.
- Exploring the selectivity of Ag-NPs towards detection of Cr^{6+} carcinogenic ions in aqueous mediums.

CHAPTER 2

MATERIALS AND METHODS

2.1 MATERIALS USED

Precursor solution of AgNO₃ (1.0 mM) was prepared by dissolving 34 mg of AgNO₃ salt into 200 mL of ultrapure (UP) water (resistivity 18.2 MΩ·cm). The flowers of *Plumeria Obtusa* plant were picked from the campus of Delhi Technological University, Delhi. The metal salts nickel perchlorate hexahydrate, copper perchlorate hydrate, cobalt perchlorate hydrate, zinc perchlorate hexahydrate, aluminium perchlorate nonahydrate, potassium dichromate, cadmium chloride hydrate, lead perchlorate trihydrate, iron perchlorate hydrate, mercury nitrate monohydrate for Ni²⁺, Cu²⁺, Co²⁺, Zn²⁺, Al³⁺, Cr⁶⁺, Cd²⁺, Pb²⁺, Fe³⁺, Fe²⁺, Hg²⁺ metal ions respectively, were bought from Sigma Aldrich.

2.2 PREPARATION OF PLANT EXTRACT

The flowers of *Plumeria obtusa* were plucked and put inside an oven for about 2 hrs at 90 °C for drying. The dehydrated flowers were pulverized using porcelain mortar and pestle. 1 gm of this powder was added to 20 mL UP water and stirred at 60 °C for 20 min. The resulting liquid was filtered to obtain an extract of dark yellowish colour. This extract was used throughout this study for preparing samples of Ag-NPs, stored in a cool and dark environment.

2.3 SYNTHESIS OF Ag-NPs

For synthesizing Ag-NPs, the precursor solution of AgNO₃ (10 mL) was augmented with the prepared flower extract (0.5 mL) and stirred for 20 min at 250 rpm at 70°C. The obtained solution was initially colourless but gradually changed to a reddish-brown tint, no further

modification in colour intensity was observed after 60 min. A schematic representation of the preparation of flower extract and the synthesis process by green route is given in Figure 2.

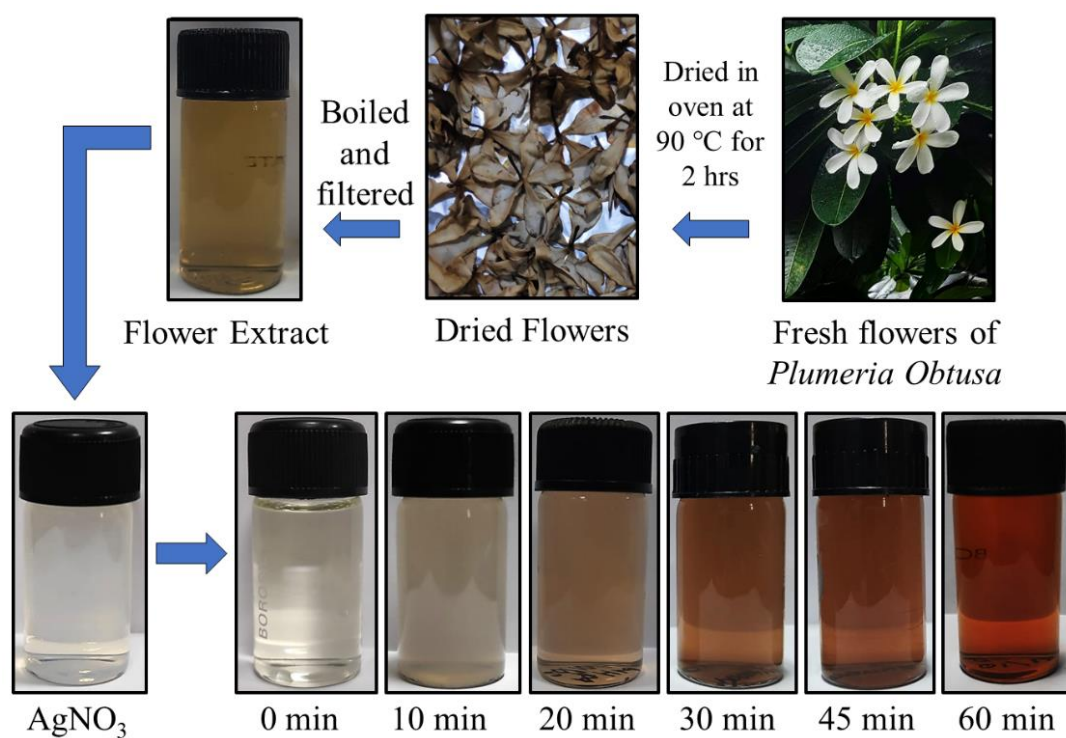


Figure 2. Biosynthesis of Ag-NPs from prepared flower essence of *Plumeria Obtusa*

CHAPTER 3

CHARACTERIZATION TECHNIQUES

3.1 UV/VIS/NIR SPECTROSCOPY

The absorption spectra for Ag-NPs were recorded using Lambda™ 750 UV/Vis/NIR spectrophotometer from PerkinElmer, shown in Figure 3. The observations were taken in the range 250 nm to 800 nm.

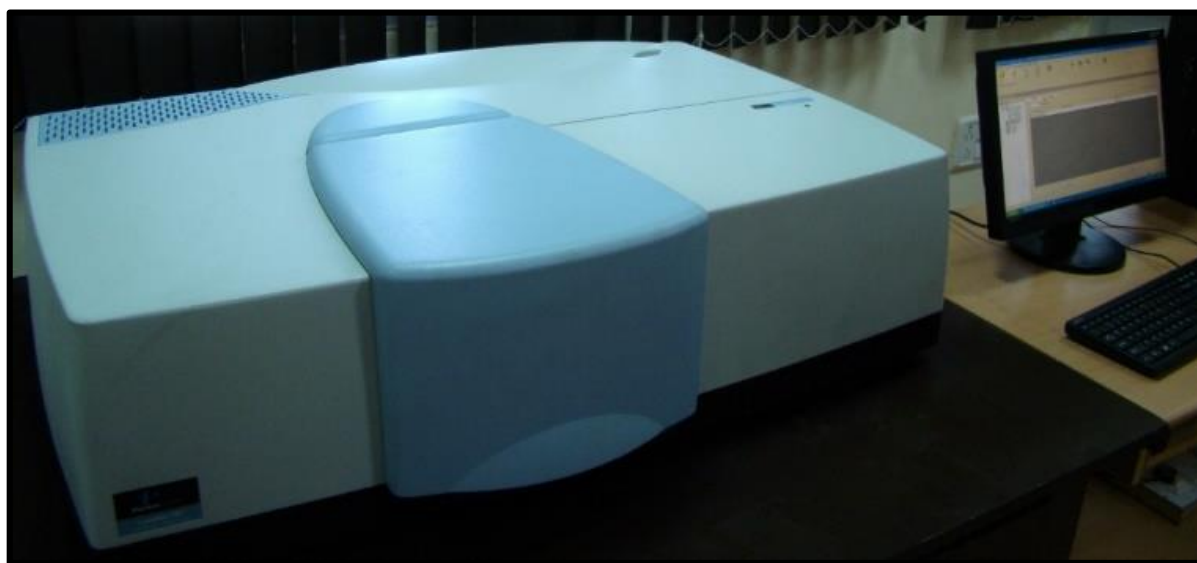


Figure 3. PerkinElmer Lambda™ 750 UV/Vis/NIR spectrophotometer

3.2 X-RAY DIFFRACTION

X-Ray Diffraction (XRD) pattern for thin films of Ag-NPs was recorded by Bruker D-8 Advanced, shown in Figure 4. The crystallite size was estimated from the following equation by Debye-Scherrer [42]:

$$D = \frac{k\lambda}{\beta \cos \theta}$$

Where, k → shape factor (0.9 for spherical configuration)

λ → wavelength of X-Ray used (0.154 nm for Cu/K α source)

β → FWHM (full width at half maximum)

$\theta \rightarrow$ Bragg's angle

The crystallite size is $\sqrt{2}$ times the particle diameter for a FCC crystal.

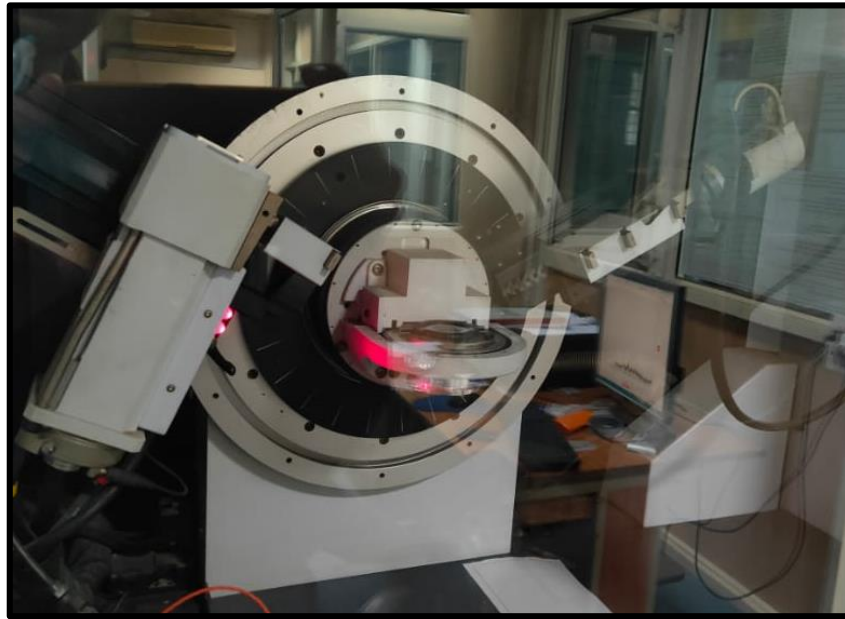


Figure 4. Bruker's D-8 Advanced X-Ray Diffractometer

3.3 TEM Analysis

For morphological and particle size analysis, TEM was performed using Morgagni 268D, shown in Figure 5.



Figure 5. Morgagni 268D Transmission Electron Microscope

3.4 ZETA POTENTIAL

The hydrodynamic size and zeta potential value of synthesised Ag-NPs in colloidal solution is analysed using Zetasizer Nano ZS by Malvern, shown in Figure 6.



Figure 6. Zetasizer Nano ZS by Malvern

CHAPTER 4

RESULT AND DISCUSSION

4.1 ABSORPTION SPECTRA

The absorption spectra were recorded for the prepared plant extracts, AgNO₃ and Ag-NPs in the range 250-800 nm since Ag-NPs show a characteristic peak around 430 nm corresponding to their SPR. Any broadening or shift of the SPR peak towards the red or blue end of wavelength spectrum due to changes in extract concentration used, reaction time, pH and temperature were studied, indicating changes in particle size or shape [43]. The same has been represented in Figure 7. Presence of just one SPR peak indicates the production of Ag-NPs of spherical conformation [44].

4.1.1 Influence of amount of flower extract on synthesis

The impact of amount of flower extract used in synthesizing Ag-NPs was inspected by taking different concentration ratios (v/v), i.e., 0.5:20, 1.0:20, 1.5:20, 2.0:20 (mL:mL) of extract to precursor solution of AgNO₃. A clear rise in absorption intensity and red shift is observed in the SPR band as the amount of flower extract increases. The rise in absorption intensity with increase in the amount of extract used is due to the rise in production of Ag-NPs due to the availability of more reduction and capping agents from extract, and the red shift indicates an increase in particle size [45].

4.1.2 Influence of time

After adding flower extract in AgNO₃, the resulting solution started changing from colourless to a pale yellow colour. The gradual colour changes can be observed by naked eyes and can be taken as a visual indicator of the synthesis process. The absorption spectra was recorded for 60 min. As time proceeds, the reaction between the phytochemicals of plant extract and AgNO₃ also proceeds forward and hence, the absorption peak rises. A blue shift is also observed with proceeding time, indicating decrease in particle size. The prepared flower extract ultimately

reduced Ag^+ ions to metallic Ag^0 in about 60 min and capped them to form Ag-NPs, as no colour change was observed beyond this.

4.1.3 Influence of temperature

The biosynthesized Ag-NPs were refrigerated (as cold as 15°C) and heated (as hot as 55°C) to observe how temperature variations influence the size distribution or polydispersity of Ag-NPs. Theoretically, the particle size is believed to decrease with increasing temperature because of nucleation being favoured at higher temperatures [46]. However, no noteworthy changes in absorption spectra were observed in this case, reflecting the high stability of prepared Ag-NPs to temperature variations.

4.1.4 Influence of pH

The pH of biosynthesized Ag-NPs was varied between 3-11 to observe the corresponding changes in size or shape of particles. Changing the pH of the reaction directly alters the electrical charges present on various phytochemicals and biomolecules, which in turn alters the rate of reduction and capping in the biosynthesis of Ag-NPs [47]. We observe that on increasing the pH from 3 to 11, a red shift is observed in SPR peak from 416 nm to 445 nm, suggesting an increase in the size of Ag-NPs. As the particle size increases, the amount of energy necessary for exciting surface plasmons reduces, thus, causing a red shift [48]. Apart from affecting particle size and the position of SPR peak, pH variation also altered the absorbance intensity. With the increase in pH, the absorbance intensity also rose significantly, indicating better reduction and capping of Ag-NPs at alkaline pH values [2,49].

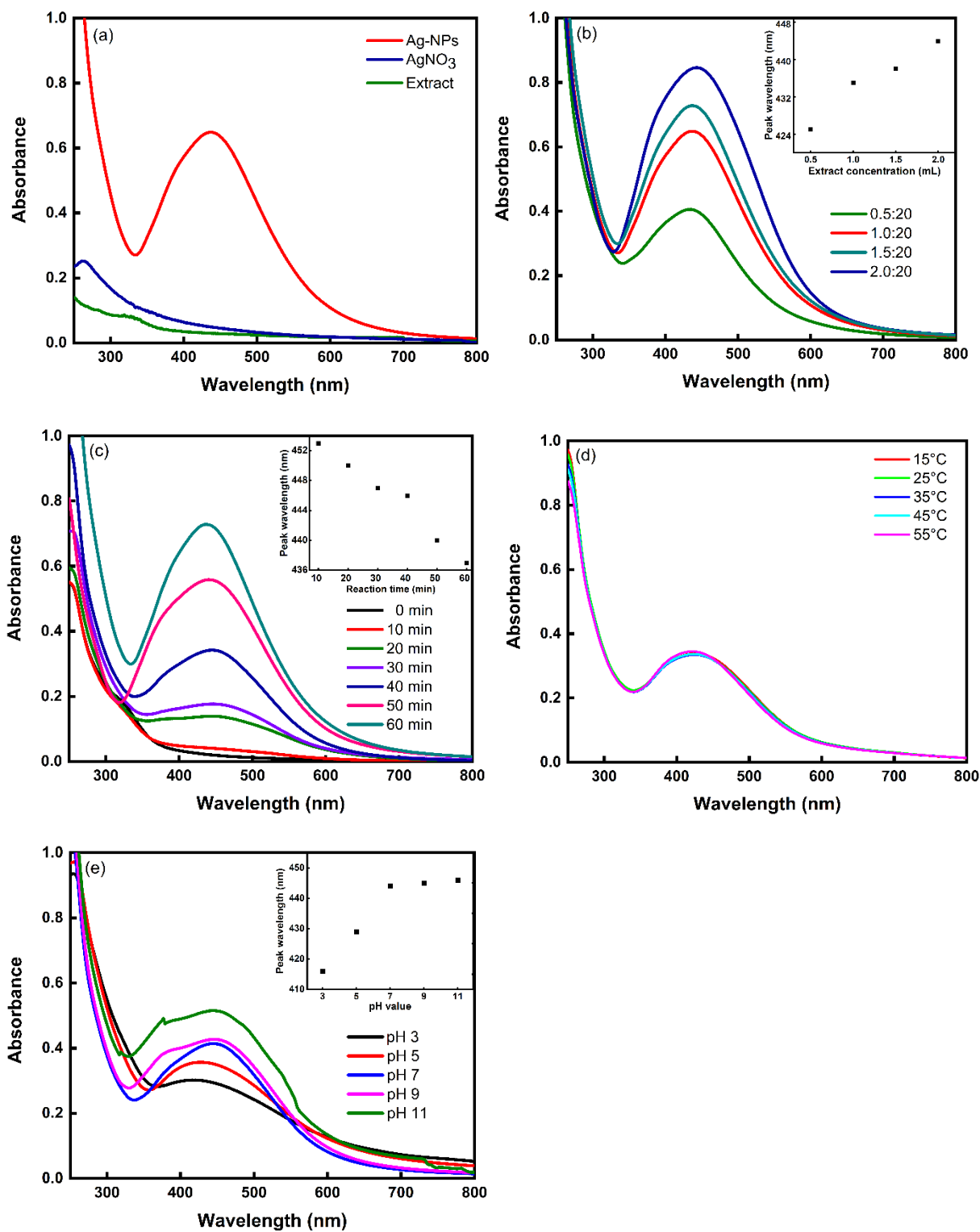


Figure 7. Absorption spectra for colloidal Ag-NPs along with AgNO₃ and prepared flower extract (a) influence of variation of extract concentration (b), the influence of time (c), the influence of temperature variation (d) and the influence of pH variation (e).

4.2 XRD PATTERN

Thin film was prepared by the drop coating technique from biosynthesized Ag-NPs for XRD analysis, given in Figure 8. Bragg's four major reflection peaks were observed at 38.19°, 46.17°, 64.96° and 76.54° representing lattice planes (111), (200), (220) and (311), confirming the lattice having a FCC (face-centered cubic) structure [50]. On comparing these observed peaks with the peak positions given in the JCPDS database for bulk silver (card no.- 04-0783), very tiny displacements may be observed that indicate the existence of strain on the formed crystal lattice, which is a typical attribute of nanocrystals [51]. Using obtained XRD pattern, the average crystallite size was also estimated, which came out to be 20 nm by adopting the Debye-Scherrer formula [42]. Since, the crystallite size is $\sqrt{2}$ times the particle diameter for a FCC crystal, the particle diameter comes out to be 14 nm.

Table 02. Bragg's reflection peaks for Ag-NPs

Lattice Plane	Peak Position
(111)	38.19°
(200)	46.17°
(220)	64.96°
(311)	76.54°

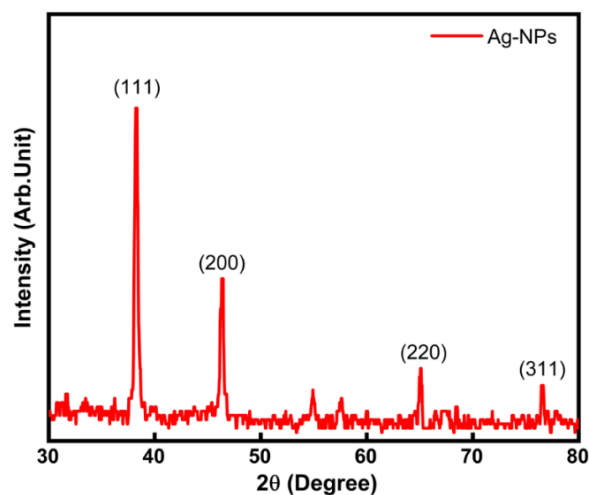


Figure 8. XRD pattern for Ag-NPs thin film.

4.3 MORPHOLOGY

To determine the morphological characteristics of biosynthesized Ag-NPs, TEM analysis was done. The sample of Ag-NPs was kept in a sonicator for 15 min. After sonicating, they were coated on a mesh grid made of copper for TEM analysis. The observed images of Ag-NPs are given in Figure 9, from which their spherical shape can be confirmed. Subsequently, a particle size distribution curve was plotted to determine the mean diameter of Ag-NPs to be 13 nm.

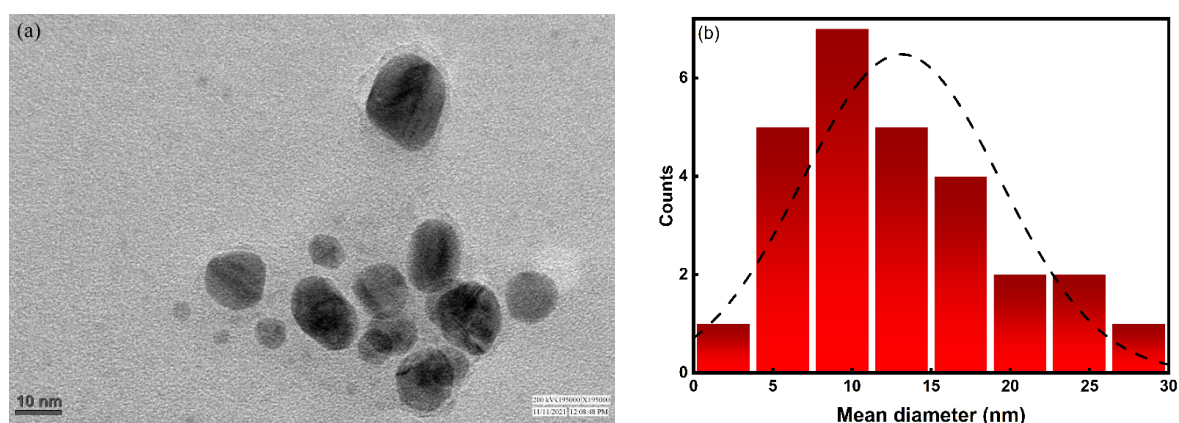


Figure 9. TEM image observed for Ag-NPs (a) Particle size distribution (b)

4.4 ZETA POTENTIAL ANALYSIS

In nanosuspensions, the creation of electrical double film at the surface leads to zeta potential directly related to its potential stability, i.e., its ability to resist coagulation. Ideally, a zeta potential value of ± 30 mV is contemplated as strongly anionic or cationic [52]. The inset of Figure 10 shows that the zeta potential of Ag-NPs comes out to be -22.7 mV (average observation of three repetitions). A negative zeta potential value indicates that the stabilizing agents controlling the resulting morphology and diameter of Ag-NPs, are anionic in nature [53]. Figure 10 shows the size distribution intensity fetched from DLS (approximately 71 nm). Since this is the hydrodynamic size, i.e., it includes the diameter of the core Ag-NPs plus the adsorbed biomolecules on the surface, this average particle size may be assumed to be much more massive than the actual size of Ag-NPs presents in prepared samples.

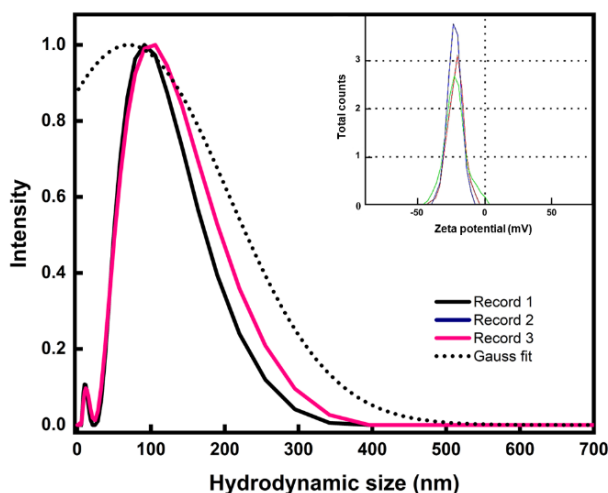


Figure 10. Hydrodynamic size distribution by intensity, repeated for 3 records. Inset represents the apparent zeta potential (mV) of colloidal Ag-NPs.

4.5 ENHANCED ANTI-BACTERIAL ACTION

Since nanoparticles have greater surface area per unit volume, they facilitate contact with the bacterial surface and enhance its antibacterial action. This was investigated using the method of disk diffusion, where the antibacterial effect of Ag-NPs was compared with that of AgNO₃ and flower extract against a gram-positive bacteria *S. Aureus*. As can be noted from Figure 11, the inhibition zone obtained for Ag-NPs is much bigger than the inhibition zone obtained for Ag-NO₃ and flower extract, thus, proving that Ag-NPs show enhanced antibacterial properties. Table 3 shows the inhibition zones obtained after treating strains of *S. Aureus* at 37 °C for 48 incubation hours.

The metallic or bulk silver is mostly inert, but the antibacterial action of AgNO₃ is accredited to the very high reactivity and binding affinity of ionized Ag particles to the proteins, DNA and RNA of bacterial cells, thus causing their malfunction. The mechanism behind the enhanced antibacterial activity of Ag-NPs is along these lines, Ag-NPs interreact with proteins and DNA of bacterial cells by penetrating the cell walls of bacteria and reaching the center. Ag-NPs facilitate rendering reactive oxygen and nitrogen species giving rise to high oxidative stress in

many cell parts, including the nucleus [19]. To protect the DNA present in nucleus, the bacteria start to agglomerate at the center, thus rupturing. Ag-NPs strike the cell division and chain of respiration of the bacteria, thus leading to total cell collapse [54].

Table 3. Inhibition zone in *S. Aureus* treated with flower extract, Ag-NPs and AgNO₃

Sample	Inhibition Zone
Ag-NPs	10.8 mm
Flower Extract	6.7 mm
AgNO ₃	7.7 mm

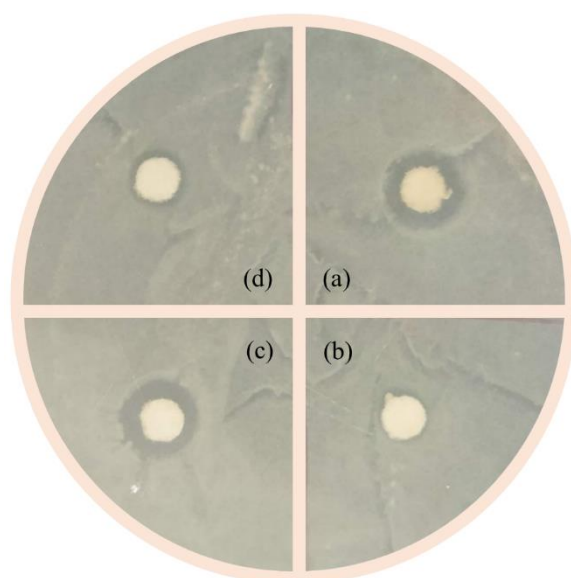


Figure 11. Antibacterial action of Ag-NPs (a), flower extract (b), Ag-NPs (c) and Ag-NO₃ against *S. Aureus* (d).

4.6 SELECTIVE SENSING TOWARDS CARCINOGENIC Cr⁶⁺

To study the potentiality of biosynthesized Ag-NPs to sense heavy metals, aqueous solutions (1μM) of various metal ions (Ni²⁺, Cu²⁺, Co²⁺, Zn²⁺, Al³⁺, Cr⁶⁺, Cd²⁺, Pb²⁺, Fe³⁺, Fe²⁺, Hg²⁺) were prepared in deionized water, to be added to Ag-NPs. On being added to the Ag-NPs sample, the resulting effect on its colour and absorption spectra was recorded. No visible colour change was recorded for any metal ions except Cr⁶⁺, as shown in Figure 12. This selectivity

makes Ag-NPs ideal for colorimetric detection of carcinogenic Cr^{6+} in aqueous mediums. The absorption spectra were also recorded to study consequent changes after treating Ag-NPs with different metal ions, shown in Figure 13 (a). On the addition of Cr^{6+} in Ag-NPs, a major fall in absorbance (absorption intensity) of the SPR band of Ag-NPs is seen. Another peak rises in the absorption spectrum at 377 nm, which is a characteristic peak of dichromate ions. For rest metal ions, minor insignificant shifts in peak absorbance intensities are recorded; a comparative bar diagram to highlight the same has been represented in inset of Figure 13 (a). To formulate controlled selective sensing of Cr^{6+} ions, Ag-NPs were treated with different concentrations of Cr^{6+} ions (1 μL to 500 μL , i.e., 0.3 nM to 166.6 nM) and their resulting absorption spectra were recorded, as given in Figure 13 (b). The reciprocal of absorbance of the SPR peak of Cr^{6+} treated Ag-NPs was plotted as a function of the concentration of Cr^{6+} and was found to be linear with a correlation factor of 0.98, given in the inset of Figure 13 (b). The slope of this linear graph was used to calculate LoD, using the formula $3.3 \times (\sigma/\text{slope})$, where σ is the standard deviation (in data repeated for 10 absorbance values). The LoD came out to be 95 ± 02 pM, which is the lowest LoD ever achieved for detecting Cr^{6+} via biosynthesized nanomaterials, to the best of our knowledge. A comparative summary to support the same has been given in Table 5. To further study the applicability of the detection method of Cr^{6+} via Ag-NPs in different aqueous mediums, two different water samples (tap water and Yamuna river water) were tested, for which the LoD came out to be almost similar, i.e., 97 and 117 pM respectively, given in Table 4. Thus, we can conclude that detection of Cr^{6+} via Ag-NPs works effectively in different aqueous mediums, given in Figure 13 (c and d).

The proposed mechanism behind the selectivity of Ag-NPs towards sensing of Cr^{6+} ions may be attributed to the contrasting electrochemical characteristics of Ag^0 and Cr^{6+} . A metal that has a greater reduction potential, i.e., Cr^{6+} (+1.33 V) can oxidize a metal with a lower reduction potential, i.e., Ag^0 (+0.80 V), whereas Cr^{2+} (-0.91 V), Cr^{3+} (-0.74 V) or any of the metals

mentioned above cannot. Thus, Cr^{6+} ions cause oxidation of Ag^0 to Ag^+ . Moreover, Ag^+ ions show strong selectivity and binding affinity to dichromate $(\text{Cr}_2\text{O}_7)^{2-}$ ions, leading to the formation of $\text{Ag}_2\text{Cr}_2\text{O}_7$ [55]. This causes the SPR band of Ag-NPs to diminish.

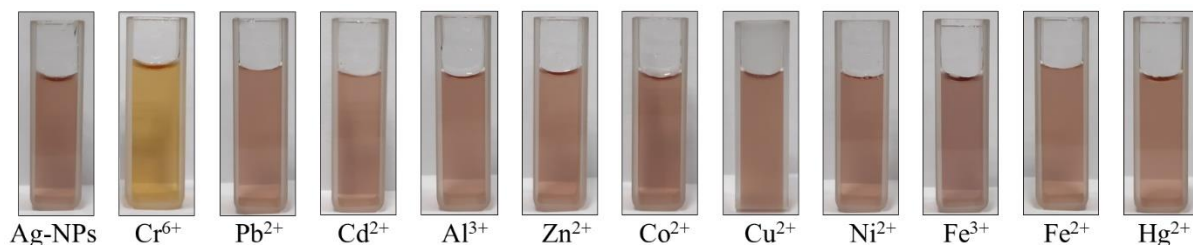


Figure 12. Colour changes in colloidal Ag-NPs after adding different metal ions (166.6 nM)

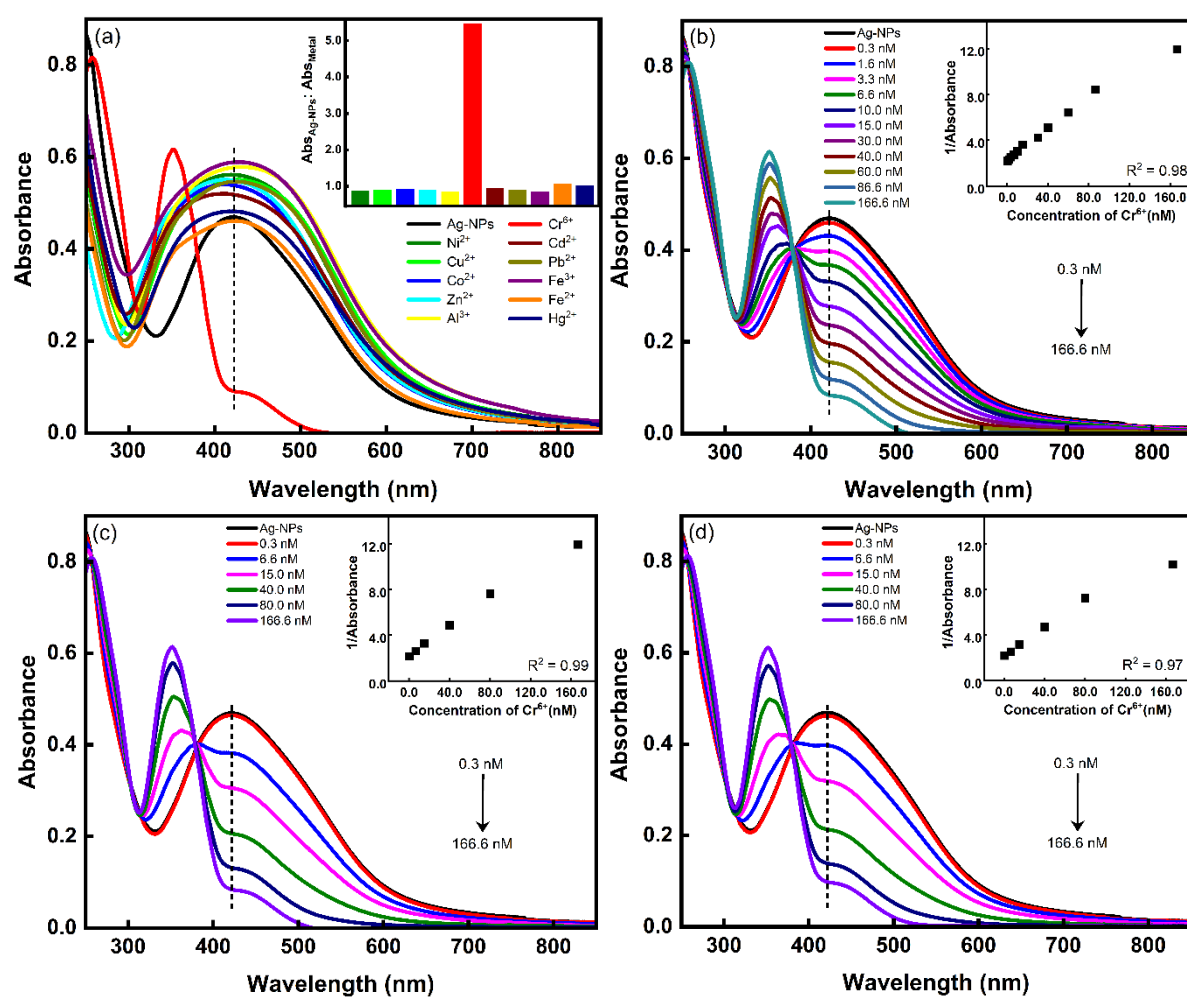


Figure 13. Absorption spectra of colloidal Ag-NPs post addition of various metal ions, inset represents a bar diagram for ratio of peak absorbances of different metal ions to pure Ag-NPs (a), successive addition of Cr^{6+} ions in aqueous medium of deionized water (b), tap water (c) and Yamuna river water (d). Inset shows linearity of $1/\text{absorbance}$ of Cr^{6+} treated Ag-NPs as a function of concentration of Cr^{6+} .

Table 4. Correlation factor and LoD for detection of Cr⁶⁺ in different aq. mediums

Aqueous Medium	Correlation factor	LoD
Deionized water	0.98	95
Tap water	0.99	97
Yamuna water	0.97	117

Table 5. Comparison of previously reported nanosensors for Cr⁶⁺ detection.

Probe used	Detection method	Linear Range	LoD	Reference
Biosynthesized Ag-NPs	SPR based	0.3-166.6 pM	95 pM	This work
Biosynthesized Ag-NPs	SPR based	10-100 ppm	0.1 ppm	[55]
Tartaric acid capped Ag-NPs	SPR based	10-100 µg/L	3 µg/L	[56]
Ascorbic acid capped Ag-NPs	SPR based	7.0×10 ⁻⁸ - 1.84×10 ⁻⁶ M	5×10 ⁻⁸ µM	[57]
Electrodeposited Au-NPs	Voltammetric	10 µg/L – 5 mg/L	5µg/L	[58]
DTT functionalized Au-NPs	SPR based	100-600 nM	20 nM	[59]
Glutathione capped CdTe QDs	Fluorescence based	0.01-1.00 µg/mL	0.008 µg/mL	[60]
Tb/acac/PAM composite NPs	Fluorescence based	5-600 ng/mL	0.8 ng/mL	[61]
Chemically synthesized Ag-NPs	SPR based	10 ⁻³ -10 ⁻⁹ M	1 nM	[62]
Tetraphenylbenzsilole derivative (TPBS-C)	Electroluminescence based	10 ⁻¹² -10 ⁻⁴ M	0.83 pM	[63]
Metal-organic complex of Cu(II)	Fluorescence-based	-	74.4 pM	[64]
TiO ₂ @Ag-NPs substrate	Surface enhanced Raman scattering	10 nm – 2 µM	1.45 nM	[65]

CHAPTER 5

CONCLUSION

Biocompatible spherical Ag-NPs were successfully synthesized where leaf extract of *Crinum asiaticum* and flower extract of *Plumeria Obtusa* served as reducer and stabilizer. The procured Ag-NPs were characterized and confirmed via various characterization techniques. The average size obtained from particle size distribution curve TEM and the XRD pattern agreed with each other. The synthesis yield was found to be significantly dependent on various physicochemical criteria such as pH, temperature, time and added extract's amount. Biosynthesized Ag-NPs act as efficient catalysts in degradation of toxic dye like Methylene Blue. They also showed enhanced anti-bacterial action over AgNO₃ against a gram-positive bacteria, *S. Aureus*. Ag-NPs were found to be very sensitive to Cr⁶⁺ ions (even for amounts as low as 1 μ L) in aqueous mediums with a very efficient LoD of 95 \pm 2 pM. Therefore, we can conclude that along with having unique optical and chemical properties, low cost, one-step simple eco-friendly synthesis procedure and biocompatibility, the synthesized Ag-NPs show efficient catalytic properties, excellent selectivity towards detecting a carcinogen (Cr⁶⁺) and appreciable antibacterial action (against *S. Aureus*), proposing to be highly useful in the fields of catalysts, biosensing and biomedicine.

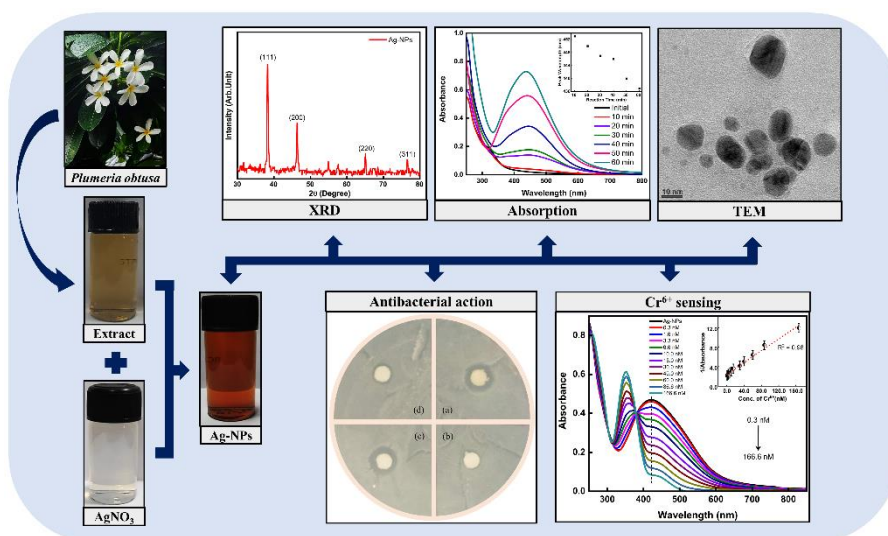


Figure. 14 Graphical Abstract

APPENDIX: SUPPLEMENTARY DATA

EDX Analysis:

Energy dispersive X-Ray (EDX) analysis was also done for confirming the presence and relative abundance of Ag-NPs in the sample. The chemical composition revealed by EDX, shown in Figure SD₁, demonstrates an appreciable amount of Ag present in the sample, along with O, C and N that are from organic agents [66] used for capping and are still bound to the surface of Ag-NPs. Table SD₁ represents chemical composition of sample.

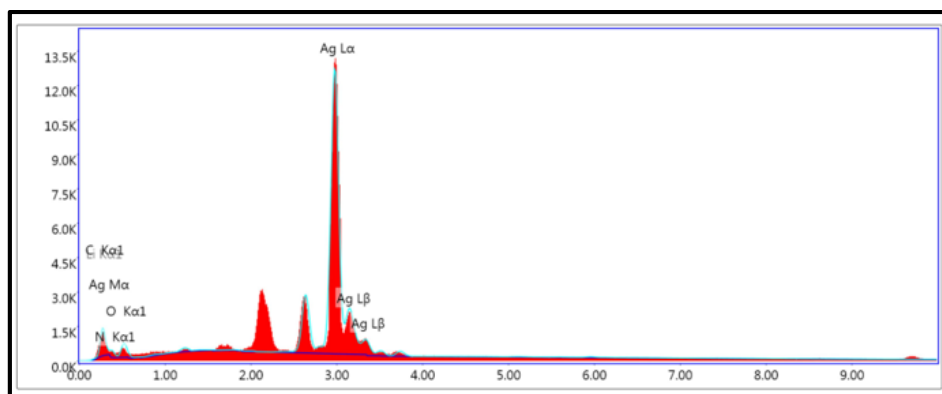


Figure SD₁. EDAX for synthesized Ag-NPs

Table SD₁. Parameters of Ag-NPs recorded on thin film

Element	Weight %	Atomic %
Ag	91.66	58.88
C	2.79	16.12
N	1.00	4.95
O	4.49	19.43

RESEARCH PAPER

1. Published article “Catalytic activity of silver nanoparticles synthesized using *Crinum asiaticum* (Sudarshan) leaf extract”

Outline

- Abstract
- Abbreviations
- Keywords
- 1. Introduction
- 2. Materials and methods
- 3. Characterization
- 4. Results and discussion
- 5. Catalytic dye degradation of methylene blue
- 6. Conclusion

Declaration of Competing Interest

Acknowledgement

References

Show full outline

Cited By (0)

Figures (13)

materialstoday:
PROCEEDINGS
Volume 56, Part 6, 2022, Pages 3714-3720

Catalytic activity of silver nanoparticles synthesized using *Crinum asiaticum* (Sudarshan) leaf extract

Samiksha Shukla¹, Anne Masih¹, Aryan, Mohan Singh Mehata[✉]

Show more

+ Add to Mendeley Share Cite

<https://doi.org/10.1016/j.matpr.2021.12.468> Get rights and content

Abstract

Synthesizing silver nanoparticles (Ag-NPs) from the green route has been gaining momentum in recent years since it is an eco-friendly, cost-efficient, non-toxic and straightforward use of precursors. The study presents a green route to synthesize Ag-NPs using green leaves of *Crinum asiaticum* and examines how biomolecules present in *Crinum asiaticum* lead to the formation of Ag-NPs. Biosynthesized Ag-NPs were confirmed, and the effect of varying pH, reaction temperature and plant

2. Article under review “Selective picomolar detection of carcinogenic chromium ions using biosynthesized silver nanoparticles and their enhanced antibacterial activity”

Track your submission

This is a new submission-tracking service. Is this helpful? Yes No

Peer review status

Selective picomolar detection of carcinogenic chromium ions using biosynthesized silver nanoparticles and their enhanced antibacterial activity

Under Review
Last review activity: 8th May 2022

- Reviews completed: 1
- Review invitations accepted: 2+
- Review invitations sent: 2+

Journal: Materials Today Sustainability

Corresponding author: Mohan Mehata

First author: Samiksha Shukla

Date of submission: 24th April 2022

Manuscript number: MTSUS-D-22-00342

REFERENCES

- [1] M.S. Mehata, Green route synthesis of silver nanoparticles using plants/ginger extracts with enhanced surface plasmon resonance and degradation of textile dye, *Mater. Sci. Eng. B.* 273 (2021) 115418–115427. <https://doi.org/10.1016/j.mseb.2021.115418>.
- [2] S. Jain, M.S. Mehata, Medicinal Plant Leaf Extract and Pure Flavonoid Mediated Green Synthesis of Silver Nanoparticles and their Enhanced Antibacterial Property., *Sci. Rep.* 7 (2017) 15867–15880. <https://doi.org/10.1038/s41598-017-15724-8>.
- [3] A. Verma, M.S. Mehata, Controllable synthesis of silver nanoparticles using Neem leaves and their antimicrobial activity, *J. Radiat. Res. Appl. Sci.* 9 (2016) 109–115. <https://doi.org/10.1016/j.jrras.2015.11.001>.
- [4] Aryan, Ruby, M.S. Mehata, Green synthesis of silver nanoparticles using *Kalanchoe pinnata* leaves (life plant) and their antibacterial and photocatalytic activities, *Chem. Phys. Lett.* 778 (2021) 138760–138770. <https://doi.org/10.1016/j.cplett.2021.138760>.
- [5] D. Garibo, H.A. Borbón-Nuñez, J.N.D. de León, E. García Mendoza, I. Estrada, Y. Toledano-Magaña, H. Tiznado, M. Ovalle-Marroquin, A.G. Soto-Ramos, A. Blanco, J.A. Rodríguez, O.A. Romo, L.A. Chávez-Almazán, A. Susarrey-Arce, Green synthesis of silver nanoparticles using *Lysiloma acapulcensis* exhibit high-antimicrobial activity., *Sci. Rep.* 10 (2020) 12805–12186. <https://doi.org/10.1038/s41598-020-69606-7>.
- [6] M. Riaz, V. Mutreja, S. Sareen, B. Ahmad, M. Faheem, N. Zahid, G. Jabbour, J. Park, Exceptional antibacterial and cytotoxic potency of monodisperse greener AgNPs prepared under optimized pH and temperature., *Sci. Rep.* 11 (2021) 2866–2877. <https://doi.org/10.1038/s41598-021-82555-z>.
- [7] K.L. Kelly, E. Coronado, L.L. Zhao, G.C. Schatz, The Optical Properties of Metal Nanoparticles: The Influence of Size, Shape, and Dielectric Environment, *J. Phys. Chem. B.* 107 (2003) 668–677. <https://doi.org/10.1021/jp026731y>.

- [8] N.T. Nandhini, S. Rajeshkumar, S. Mythili, The possible mechanism of eco-friendly synthesized nanoparticles on hazardous dyes degradation, *Biocatal. Agric. Biotechnol.* 19 (2019) 101138–101148. <https://doi.org/10.1016/j.bcab.2019.101138>.
- [9] J.H. Jung, H. Cheol Oh, H. Soo Noh, J.H. Ji, S. Soo Kim, Metal nanoparticle generation using a small ceramic heater with a local heating area, *J. Aerosol Sci.* 37 (2006) 1662–1670. <https://doi.org/10.1016/j.jaerosci.2006.09.002>.
- [10] A. Shenava, Synthesis of Silver Nanoparticles By Chemical Reduction Method and Their Antifungal Activity, *Int. Res. J. Pharm.* 4 (2013) 111–113. <https://doi.org/10.7897/2230-8407.041024>.
- [11] A. Bala, G. Rani, A review on phytosynthesis, affecting factors and characterization techniques of silver nanoparticles designed by green approach, *Int. Nano Lett.* 10 (2020) 159–176. <https://doi.org/10.1007/s40089-020-00309-7>.
- [12] S. Ghosh, R. Ahmad, K. Banerjee, M.F. AlAjmi, S. Rahman, Mechanistic Aspects of Microbe-Mediated Nanoparticle Synthesis., *Front. Microbiol.* 12 (2021) 638068–638080. <https://doi.org/10.3389/fmicb.2021.638068>.
- [13] Y. Park, Y.N. Hong, A. Weyers, Y.S. Kim, R.J. Linhardt, Polysaccharides and phytochemicals: a natural reservoir for the green synthesis of gold and silver nanoparticles., *IET Nanobiotechnology.* 5 (2011) 69–78. <https://doi.org/10.1049/iet-nbt.2010.0033>.
- [14] S.G. Velhal, S.D. Kulkarni, R. V. Latpate, Fungal mediated silver nanoparticle synthesis using robust experimental design and its application in cotton fabric, *Int. Nano Lett.* 6 (2016) 257–264. <https://doi.org/10.1007/s40089-016-0192-9>.
- [15] J.W. Alexander, History of the Medical Use of Silver, *Surg. Infect. (Larchmt).* 10 (2009) 289–292. <https://doi.org/10.1089/sur.2008.9941>.
- [16] S. Medici, M. Peana, V.M. Nurchi, M.A. Zoroddu, Medical Uses of Silver: History,

- Myths, and Scientific Evidence, *J. Med. Chem.* 62 (2019) 5923–5943.
<https://doi.org/10.1021/acs.jmedchem.8b01439>.
- [17] F.A. Alharthi, A.A. Alghamdi, N. Al-Zaqri, H.S. Alanazi, A.A. Alsyahi, A. El Marghany, N. Ahmad, Facile one-pot green synthesis of Ag-ZnO Nanocomposites using potato peel and their Ag concentration dependent photocatalytic properties., *Sci. Rep.* 10 (2020) 20229–20243. <https://doi.org/10.1038/s41598-020-77426-y>.
- [18] M. Parthibavarman, S. Bhuvaneshwari, M. Jayashree, R. Boopathi Raja, Green Synthesis of Silver (Ag) Nanoparticles Using Extract of Apple and Grape and with Enhanced Visible Light Photocatalytic Activity, *Bionanoscience.* 9 (2019) 423–432.
<https://doi.org/10.1007/s12668-019-0605-0>.
- [19] Ruby, Aryan, M.S. Mehata, Surface plasmon resonance allied applications of silver nanoflowers synthesized from: *Breynia vitis-idaea* leaf extract, *Dalt. Trans.* 51 (2022) 2726–2736. <https://doi.org/10.1039/d1dt03592d>.
- [20] S. Shrivastava, T. Bera, S.K. Singh, G. Singh, P. Ramachandrarao, D. Dash, Characterization of antiplatelet properties of silver nanoparticles., *ACS Nano.* 3 (2009) 1357–1364. <https://doi.org/10.1021/nn900277t>.
- [21] B. Pant, P.S. Saud, M. Park, S.-J. Park, H.-Y. Kim, General one-pot strategy to prepare Ag–TiO₂ decorated reduced graphene oxide nanocomposites for chemical and biological disinfectant, *J. Alloys Compd.* 671 (2016) 51–59.
<https://doi.org/10.1016/j.jallcom.2016.02.067>.
- [22] M. Ramesh, M. Anbuvaran, G. Viruthagiri, Green synthesis of ZnO nanoparticles using *Solanum nigrum* leaf extract and their antibacterial activity, *Spectrochim. Acta Part A Mol. Biomol. Spectrosc.* 136 (2015) 864–870. <https://doi.org/10.1016/j.saa.2014.09.105>.
- [23] P. Le Thi, Y. Lee, H.J. Kwon, K.M. Park, M.H. Lee, J.-C. Park, K.D. Park, Tyrosinase-mediated surface coimmobilization of heparin and silver nanoparticles for

- antithrombotic and antimicrobial activities., *ACS Appl. Mater. Interfaces*. 9 (2017) 20376–20384. <https://doi.org/10.1021/acsami.7b02500>.
- [24] H. Agarwal, S.V. Kumar, S. Rajeshkumar, Antidiabetic effect of silver nanoparticles synthesized using lemongrass (*Cymbopogon citratus*) through conventional heating and microwave irradiation approach, *J. Microbiol. Biotechnol. Food Sci.* 7 (2018) 371–376. <https://doi.org/10.15414/jmbfs.2018.7.4.371-376>.
- [25] E. Liu, M. Zhang, H. Cui, J. Gong, Y. Huang, J. Wang, Y. Cui, W. Dong, L. Sun, H. He, V.C. Yang, Tat-functionalized Ag-Fe₃O₄ nano-composites as tissue-penetrating vehicles for tumor magnetic targeting and drug delivery, *Acta Pharm. Sin. B.* 8 (2018) 956–968. <https://doi.org/10.1016/j.apsb.2018.07.012>.
- [26] H. Gao, Progress and perspectives on targeting nanoparticles for brain drug delivery, *Acta Pharm. Sin. B.* 6 (2016) 268–286. <https://doi.org/10.1016/j.apsb.2016.05.013>.
- [27] G. Yamal, P. Sharmila, K.S. Rao, P. Pardha-Saradhi, Inbuilt potential of YEM medium and its constituents to generate Ag/Ag₂O nanoparticles, *PLoS One*. 8 (2013) e61750-61760. <https://doi.org/10.1371/journal.pone.0061750>.
- [28] T. Bihani, P. Tandel, J. Wadekar, *Plumeria obtusa* L.: A systematic review of its traditional uses, morphology, phytochemistry and pharmacology, *Phytomedicine Plus*. 1 (2021) 100052. <https://doi.org/10.1016/j.phyplu.2021.100052>.
- [29] S. Semenya, M. Potgieter, L. Erasmus, Ethnobotanical survey of medicinal plants used by Bapedi healers to treat diabetes mellitus in the Limpopo Province, South Africa, *J. Ethnopharmacol.* 141 (2012) 440–445. <https://doi.org/10.1016/j.jep.2012.03.008>.
- [30] O. Kaisoon, S. Siriamornpun, N. Weerapreeyakul, N. Meeso, Phenolic compounds and antioxidant activities of edible flowers from Thailand, *J. Funct. Foods*. 3 (2011) 88–99. <https://doi.org/10.1016/j.jff.2011.03.002>.
- [31] M. Saleem, N. Akhtar, N. Riaz, M.S. Ali, A. Jabbar, Isolation and characterization of

- secondary metabolites from *Plumeria obtusa*, *J. Asian Nat. Prod. Res.* 13 (2011) 1122–1127. <https://doi.org/10.1080/10286020.2011.618452>.
- [32] H.S. Kim, Y.J. Kim, Y.R. Seo, An Overview of Carcinogenic Heavy Metal: Molecular Toxicity Mechanism and Prevention, *J. Cancer Prev.* 20 (2015) 232–240. <https://doi.org/10.15430/JCP.2015.20.4.232>.
- [33] A.J. Paine, Mechanisms of chromium toxicity, carcinogenicity and allergenicity: Review of the literature from 1985 to 2000, *Hum. Exp. Toxicol.* 20 (2001) 439–451. <https://doi.org/10.1191/096032701682693062>.
- [34] I.B. Weinstein, The scientific basis for carcinogen detection and primary cancer prevention., *Cancer.* 47 (1981) 1133–1141. [https://doi.org/10.1002/1097-0142\(19810301\)47:5+<1133::aid-cnrcr2820471312>3.0.co;2-7](https://doi.org/10.1002/1097-0142(19810301)47:5+<1133::aid-cnrcr2820471312>3.0.co;2-7).
- [35] J. Ashby, R.S. Morrod, Detection of human carcinogens., *Nature.* 352 (1991) 185–186. <https://doi.org/10.1038/352185a0>.
- [36] R. Nusko, K.G. Heumann, Cr(III)/Cr(VI) speciation in aerosol particles by extractive separation and thermal ionization isotope dilution mass spectrometry, *Fresenius. J. Anal. Chem.* 357 (1997) 1050–1055. <https://doi.org/10.1007/s002160050303>.
- [37] M. Sperling, S. Xu, B. Welz, Determination of Chromium (III) and Chromium (VI) in Water Using Flow Injection On-Line Preconcentration with Selective Adsorption on Activated Alumina and Flame Atomic Absorption Spectrometric Detection, *Anal. Chem.* 64 (1992) 3101–3108. <https://doi.org/10.1021/ac00048a007>.
- [38] S. Balasubramanian, V. Pugalenti, Determination of total chromium in tannery waste water by inductively coupled plasma-atomic emission spectrometry, flame atomic absorption spectrometry and UV-visible spectrophotometric methods, *Talanta.* 50 (1999) 457–467. [https://doi.org/10.1016/S0039-9140\(99\)00135-6](https://doi.org/10.1016/S0039-9140(99)00135-6).
- [39] E.J. Arar, J.D. Pfaff, Determination of dissolved hexavalent chromium in industrial

- wastewater effluents by ion chromatography and post-column derivatization with diphenylcarbazide, *J. Chromatogr. A.* 546 (1991) 335–340. [https://doi.org/10.1016/S0021-9673\(01\)93031-6](https://doi.org/10.1016/S0021-9673(01)93031-6).
- [40] N.D. Nguyen, T. Van Nguyen, A.D. Chu, H.V. Tran, L.T. Tran, C.D. Huynh, A label-free colorimetric sensor based on silver nanoparticles directed to hydrogen peroxide and glucose, *Arab. J. Chem.* 11 (2018) 1134–1143. <https://doi.org/10.1016/j.arabjc.2017.12.035>.
- [41] H.K. Choi, M.-J. Lee, S.N. Lee, T.-H. Kim, B.-K. Oh, Noble Metal Nanomaterial-Based Biosensors for Electrochemical and Optical Detection of Viruses Causing Respiratory Illnesses, *Front. Chem.* 9 (2021) 605–605. <https://doi.org/10.3389/fchem.2021.672739>.
- [42] A.O. Bokuniaeva, A.S. Vorokh, Estimation of particle size using the Debye equation and the Scherrer formula for polyphasic TiO₂ powder, *J. Phys. Conf. Ser.* 1410 (2019) 012057–012064. <https://doi.org/10.1088/1742-6596/1410/1/012057>.
- [43] S.L. Smitha, K.M. Nissamudeen, D. Philip, K.G. Gopchandran, Studies on surface plasmon resonance and photoluminescence of silver nanoparticles., *Spectrochim. Acta. A. Mol. Biomol. Spectrosc.* 71 (2008) 186–90. <https://doi.org/10.1016/j.saa.2007.12.002>.
- [44] B.J. Wiley, S.H. Im, Z.Y. Li, J. McLellan, A. Siekkinen, Y. Xia, Maneuvering the surface plasmon resonance of silver nanostructures through shape-controlled synthesis, *J. Phys. Chem. B.* 110 (2006) 15666–15675. <https://doi.org/10.1021/jp0608628>.
- [45] K.C. Lee, S.J. Lin, C.H. Lin, C.S. Tsai, Y.J. Lu, Size effect of Ag nanoparticles on surface plasmon resonance, *Surf. Coatings Technol.* 202 (2008) 5339–5342. <https://doi.org/10.1016/j.surfcoat.2008.06.080>.
- [46] S. Shukla, A. Masih, Aryan, M.S. Mehata, Catalytic activity of silver nanoparticles synthesized using *Crinum asiaticum* (Sudarshan) leaf extract, *Mater. Today Proc.* (In

- press) (2022). <https://doi.org/10.1016/j.matpr.2021.12.468>.
- [47] M.M.H. Khalil, E.H. Ismail, K.Z. El-Baghdady, D. Mohamed, Green synthesis of silver nanoparticles using olive leaf extract and its antibacterial activity, *Arab. J. Chem.* 7 (2014) 1131–1139. <https://doi.org/10.1016/j.arabjc.2013.04.007>.
- [48] O.A. Yeshchenko, I.M. Dmitruk, A.A. Alexeenko, A. V. Kotko, J. Verdal, A.O. Pinchuk, Size and Temperature Effects on the Surface Plasmon Resonance in Silver Nanoparticles, *Plasmonics.* 7 (2012) 685–694. <https://doi.org/10.1007/s11468-012-9359-z>.
- [49] I. Fernando, Y. Zhou, Impact of pH on the stability, dissolution and aggregation kinetics of silver nanoparticles., *Chemosphere.* 216 (2019) 297–305. <https://doi.org/10.1016/j.chemosphere.2018.10.122>.
- [50] R.I. Priyadarshini, G. Prasannaraj, N. Geetha, P. Venkatachalam, Microwave-Mediated Extracellular Synthesis of Metallic Silver and Zinc Oxide Nanoparticles Using Macro-Algae (*Gracilaria edulis*) Extracts and Its Anticancer Activity Against Human PC3 Cell Lines, *Appl. Biochem. Biotechnol.* 174 (2014) 2777–2790. <https://doi.org/10.1007/s12010-014-1225-3>.
- [51] M.J. Hÿtch, A.M. Minor, Observing and measuring strain in nanostructures and devices with transmission electron microscopy, *MRS Bull.* 39 (2014) 138–146. <https://doi.org/10.1557/mrs.2014.4>.
- [52] S. Pattanayak, M.M.R. Mollick, D. Maity, S. Chakraborty, S.K. Dash, S. Chattopadhyay, S. Roy, D. Chattopadhyay, M. Chakraborty, Butea monosperma bark extract mediated green synthesis of silver nanoparticles: Characterization and biomedical applications, *J. Saudi Chem. Soc.* 21 (2017) 673–684. <https://doi.org/10.1016/j.jscs.2015.11.004>.
- [53] S. Singh, A. Bharti, V.K. Meena, Structural, thermal, zeta potential and electrical properties of disaccharide reduced silver nanoparticles, *J. Mater. Sci. Mater. Electron.*

- 25 (2014) 3747–3752. <https://doi.org/10.1007/s10854-014-2085-x>.
- [54] M. Rai, A. Yadav, A. Gade, Silver nanoparticles as a new generation of antimicrobials, *Biotechnol. Adv.* 27 (2009) 76–83. <https://doi.org/10.1016/j.biotechadv.2008.09.002>.
- [55] M. Ismail, M.I. Khan, K. Akhtar, M.A. Khan, A.M. Asiri, S.B. Khan, Biosynthesis of silver nanoparticles: A colorimetric optical sensor for detection of hexavalent chromium and ammonia in aqueous solution, *Phys. E Low-Dimensional Syst. Nanostructures.* 103 (2018) 367–376. <https://doi.org/10.1016/j.physe.2018.06.015>.
- [56] K. Shrivastava, S. Sahu, G.K. Patra, N.K. Jaiswal, R. Shankar, Localized surface plasmon resonance of silver nanoparticles for sensitive colorimetric detection of chromium in surface water, industrial waste water and vegetable samples, *Anal. Methods.* 8 (2016) 2088–2096. <https://doi.org/10.1039/c5ay03120f>.
- [57] X. Wu, Y. Xu, Y. Dong, X. Jiang, N. Zhu, Colorimetric determination of hexavalent chromium with ascorbic acid capped silver nanoparticles, *Anal. Methods.* 5 (2013) 560–565. <https://doi.org/10.1039/c2ay25989c>.
- [58] G. Liu, Y.Y. Lin, H. Wu, Y. Lin, Voltammetric detection of Cr(VI) with disposable screen-printed electrode modified with gold nanoparticles, *Environ. Sci. Technol.* 41 (2007) 8129–8134. <https://doi.org/10.1021/es071726z>.
- [59] F. Tan, X. Liu, X. Quan, J. Chen, X. Li, H. Zhao, Selective detection of nanomolar Cr(VI) in aqueous solution based on 1,4-dithiothreitol functionalized gold nanoparticles, *Anal. Methods.* 3 (2011) 343–347. <https://doi.org/10.1039/c0ay00534g>.
- [60] L. Zhang, C. Xu, B. Li, Simple and sensitive detection method for chromium(VI) in water using glutathione-capped CdTe quantum dots as fluorescent probes, *Microchim. Acta.* 166 (2009) 61–68. <https://doi.org/10.1007/s00604-009-0164-0>.
- [61] L. Wang, G. Bian, L. Dong, T. Xia, S. Hong, H. Chen, Selective fluorescence determination of chromium (VI) in water samples with terbium composite nanoparticles,

- Spectrochim. Acta - Part A Mol. Biomol. Spectrosc. 65 (2006) 123–126.
<https://doi.org/10.1016/j.saa.2005.09.042>.
- [62] A. Ravindran, M. Elavarasi, T.C. Prathna, A.M. Raichur, N. Chandrasekaran, A. Mukherjee, Selective colorimetric detection of nanomolar Cr (VI) in aqueous solutions using unmodified silver nanoparticles, *Sensors Actuators, B Chem.* 166–167 (2012) 365–371. <https://doi.org/10.1016/j.snb.2012.02.073>.
- [63] J. Guo, W. Feng, P. Du, R. Zhang, J. Liu, Y. Liu, Z. Wang, X. Lu, Aggregation-Induced Electrochemiluminescence of Tetraphenylbenzosilole Derivatives in an Aqueous Phase System for Ultrasensitive Detection of Hexavalent Chromium, *Anal. Chem.* 92 (2020) 14838–14845. <https://doi.org/10.1021/acs.analchem.0c03709>.
- [64] R.K. Mondal, S. Dhibar, P. Mukherjee, A.P. Chattopadhyay, R. Saha, B. Dey, Selective picomolar level fluorometric sensing of the Cr(VI)-oxoanion in a water medium by a novel metal-organic complex, *RSC Adv.* 6 (2016) 61966–61973. <https://doi.org/10.1039/c6ra12819j>.
- [65] W. Zhou, B.-C. Yin, B.-C. Ye, Highly sensitive surface-enhanced Raman scattering detection of hexavalent chromium based on hollow sea urchin-like TiO₂@Ag nanoparticle substrate., *Biosens. Bioelectron.* 87 (2017) 187–194. <https://doi.org/10.1016/j.bios.2016.08.036>.
- [66] A.G. Femi-Adepoju, A.O. Dada, K.O. Otun, A.O. Adepoju, O.P. Fatoba, Green synthesis of silver nanoparticles using terrestrial fern (*Gleichenia Pectinata* (Willd.) C. Presl.): characterization and antimicrobial studies, *Heliyon.* 5 (2019) e01543. <https://doi.org/10.1016/j.heliyon.2019.e01543>.